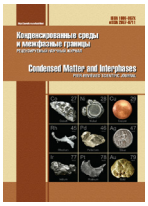

ISSN 1606-867X (Print)
ISSN 2687-0711 (Online)
Condensed Matter and Interphases
Kondensirovannye Sredy i Mezhfaznye Granitsy
https://journals.vsu.ru/kcmf/

Original articles

Research article
https://doi.org/10.17308/kcmf.2023.25/10976

Activity and stability of PtCo/C electrocatalysts for alcohol oxidation

D. K. Mauer✉, S. V. Belenov, A. Yu. Nikulin, N. V. Toporkov

Southen Federal University,
105/42 Bolshaya Sadovaya str., Rostov-on-Don 344006, Russian Federation

Abstract

This study considers the liquid-phase synthesis of PtCo/C catalysts based on CoO_x/C composite carriers with different mass fractions of metals and Pt:Co ratios. The purpose of the article is to study the activity of PtCo/C electrocatalysts of various compositions in the oxidation reactions of methanol and ethanol and to compare their characteristics with their commercial PtRu/C and Pt/C analogues.

PtCo/C catalysts were synthesised with Pt:Co ratios of 1:1 and 3:1. The specific active surface of the obtained PtCo/C materials was determined, their activity in the oxidation reactions of methanol and ethanol and their resistance to poisoning by intermediate products of alcohol oxidation were studied. The structural and electrochemical characteristics of the obtained PtCo/C catalysts were studied by X-ray diffraction, cyclic voltammetry, and chronoamperometry. It was found that PtCo/C materials with a mass fraction of platinum close to 20% are the most active and stable as compared to their commercial PtRu/C and Pt/C analogues.

The presented results show that PtCo/C catalysts are a promising material for direct alcohol fuel cells.

Keywords: Methanol fuel cells, Ethanol fuel cells, Electrocatalysis, Ethanol oxidation reaction, Methanol oxidation reaction, Bimetallic catalysts

Funding: The research was supported by the Ministry of Science and Higher Education of the Russian Federation in the framework of the government order to higher education institutions in the sphere of scientific research, project No. 0852–2020-0019.

For citation: Mauer D. K., Belenov S. V., Nikulin A.Y., Toporkov N.V. Activity and stability of PtCo/C electrocatalysts for alcohol oxidation. *Condensed Matter and Interphases*. 2023;25(1): 72–84. https://doi.org/10.17308/kcmf.2023.25/10976

Для цитирования: Мауэр Д. К., Беленов С. В., Никулин А. Ю., Топорков Н. В. Активность и стабильность PtCo/C электрокатализаторов окисления спиртов. *Конденсированные среды и межфазные границы*. 2023;25(1): 72–84. https://doi.org/10.17308/kcmf.2023.25/10976

✉ Vladislav, S. Menshikov, e-mail: men.vlad@mail.ru

1. Introduction

In recent years, fuel cell (FE) technologies, which use various alcohols as fuel, are being intensively developed. This is associated with the fact that they are highly efficient, low-emission, and easy to transport and refuel [1–5]. However, currently, such devices have a number of serious shortcomings, primarily associated with slow multistage methanol (MOR) or ethanol (EOR) oxidation reactions [6,7] and catalysts' insufficient stability and resistance to CO poisoning [8, 9]. Today, the most common catalysts for low-temperature hydrogen-air and alcohol fuel cells are platinum nanoparticles deposited on carbon black [2, 9]. However, pure platinum on a carbon carrier is not a very effective catalyst for MOR and EOR due to a rapid poisoning of its surface with CO and other products of alcohol oxidation [8–10]. Therefore, there is a need to search catalysts that would have a higher tolerance to the intermediate products of the oxidation reaction of alcohols.

One of the most promising approaches to improving the performance of catalysts is obtaining bimetallic catalysts by doping Pt with transition d-metals, such as: Co, Ni, Fe, Cu, etc. [11–16]. Increased activity of bimetallic platinum-containing electrocatalysts can be explained by geometric factors (decreased interatomic distance in the crystal lattice) [17], a change in the energy of the platinum *d*-orbitals [18], and a change in the surface morphology of the nanoparticles [19] associated with a selective dissolution of the alloying component [16]. It should be noted that currently the most effective bimetallic catalysts for MOR are PtRu/C catalysts [3]. However, they are quite costly since they contain precious metals.

It is known that Toyota uses PtCo/C catalysts in their Mirai cars [20], which proves that such systems are commercially promising. Hence, we assume that PtCo/C can also be effective for MOR and EOR. For example, the authors of [21] demonstrated that a PtCo alloy with a developed structure has a noticeably better activity in MOR in terms of mass activity, electrochemical surface area (ESA), the potential for the methanol oxidation onset, and durability as compared to Pt_3Co, Pt/C, and PtRu/C catalysts. The authors of [22] claim that nanoparticles obtained by the hydrothermal synthesis of PtCo in the form of concave nanocrosses whose dimensions exceed 20 nm demonstrate high activity and stability in MOR. The comparison of PtCo/C, PtNi/C, and Pt/C catalysts in operation [23] revealed that both bimetallic catalysts show higher characteristics of stability and activity in MOR as compared to the commercial catalyst. It should also be noted that the PtCo/C catalyst has increased stability as compared to PtNi/C. It is necessary to emphasise that it is highly challenging to develop catalysts for ethanol oxidation due to a complex oxidation mechanism and a large number of intermediate products [24]. That is why multicomponent platinum-containing catalysts are often used for EOR: PtRuNi/C, PtSnRh/C, PtSn/C, CoPtAu [25–27]. The use of PtCo/C catalysts in EOR is currently under study. A number of studies have been dedicated to the activity of such catalysts in EOR [28-31]. In [28], the authors found that PtCo and PtMn electrocatalysts obtained by electrodeposition on titanium foil show the greatest activity in the methanol and ethanol oxidation reactions as compared to pure platinum. The authors of [29] studied the activity of a number of PtCo nanoparticles deposited on graphene with an atomic Pt:Co ratio of 1:1, 1:7, and 1:44 and a size of particles of 1 to 3 nm. In this study, it was found that all Pt:Co catalysts demonstrate increased activity and stability in EOR as compared to platinum nanoparticles on graphene, and the catalyst with a Pt:Co ratio of 1:7 has the best characteristics. The paper [30] compared the activity in EOR of PtCo/C materials obtained by various methods of synthesis. PtCo/C catalysts prepared with ethylene glycol and sodium borohydride used as reducing agents were found to be the most active. In [31] it was shown that catalysts in the form of Pt_1Co_1 nanowires obtained by hydrothermal synthesis demonstrate 3.69 times higher mass activity in EOR than pure Pt.

Thus, doping platinum with some d-metals is a well-known method that significantly improves the characteristics of electrocatalysts in MOR and EOR. We believe that PtCo/C catalysts may be promising materials for direct alcohol fuel cells.

Hence, the purpose of this study was to study the characteristics of PtCo/C catalysts of various compositions obtained from composite

CoO_x/C carriers and to compare them with their commercial PtRu/C and Pt/C analogues.

2. Experimental

Platinum-cobalt catalysts were obtained by borohydride synthesis from CoO_x/C carriers with a cobalt oxide content of 8% and 25% as it had been described in an earlier published study [32]. The composition and structure of CoO_x/C carriers were also presented earlier [32]. Materials obtained from the carrier with a mass fraction of cobalt oxide of 8% were designated as PC2 (PtCo composition) and PC3 (Pt_3Co composition) materials with a mass fraction of oxide of 25% were designated as PC1 (PtCo composition).

The mass fraction of metals in the obtained samples was determined by thermogravimetry based on the weight of the unburned residue. For this, a weighed portion of the studied sample was placed in a pre-calcined crucible with a constant mass and heat treated at 800 °C for 40 min. When calculating the mass fraction of Pt and PtCo, the formation of Co_3O_4 oxide was taken into account.

The Pt:Co ratio in the obtained samples was determined by X-ray fluorescence analysis (XRF) using a RFS-001 spectrometer (Research Institute of Physics, Southern Federal University, Russia). The conditions of the analysis were as follows: the X-ray tube voltage: 50 kV; current: 150 μA; anode material: molybdenum; spectrum acquisition time: 300 s. X-ray fluorescence spectra were recorded and processed using the UniveRS software (Southern Federal University, Russia).

The XRD phase composition (XRD) and the average size of crystallites were determined by powder X-ray diffraction using an ARL X'TRA diffractometer (Cu K_α). The conditions of the experiment were as follows: room temperature, an angle range of 2θ from 15 to 55 degrees. The average crystallite size was determined using the Scherrer formula [33]:

$$D = K\lambda/(\mathrm{FWHM}\cos\theta),$$

where $K = 0.98$ is the Scherrer constant, λ is the wavelength of monochromatic radiation in Å, FWHM is the full width of the peak at half maximum (in radians), D is the average crystallite size, nm; θ is the reflection angle in radians.

The electrochemical behaviour of the catalysts was studied by cyclic voltammetry (CV) and chronoamperometry using a VesaSTAT 3 potentiostat. For this study, we used a rotating disk electrode and a three-electrode cell, a platinum wire was used as a counter electrode, and a silver chloride electrode was used as a reference electrode. All potentials in this study are relative to a reversible hydrogen electrode (RHE). A weighed portion of the catalyst with a mass of 0.0060 g was placed in a mixture of 100 μl of 0.5% Nafionalcohol solution and 900 μl of isopropyl alcohol (extra pure grade). The resulting suspension was homogenised in ultrasound for 30 minutes, while making sure that the water temperature did not rise above 20 °C. Then it was stirred on a vibrating platform for 30 minutes. After that, a 6 μl aliquot of ink was applied to the end of the disk electrode and dried while rotating at room temperature.

Surface standardisation was carried out in 0.1 M electrolyte solution (Sigma Aldrich $HClO_4$) saturated with argon at atmospheric pressure, in the range of potentials of 0.04–1.20 V at a sweep rate of 100 mV/s. The electrochemical surface area was determined by the formula:

$$\mathrm{ESA}(CO_{ad}) = Q_{CO}/Rm1000,$$

where Q_{CO} is the amount of electricity spent on the oxidation of the chemisorbed CO monolayer on the voltammogramme measured at a sweep rate of 20 mV/s under similar conditions [5]; R is the amount of electricity spent on the oxidation of CO (420 μC/cm^2); and m is the mass of Pt on the electrode (g).

Catalysts' activity in MOR was evaluated in 0.1 M $HClO_4$ with the addition of a methanol solution to achieve a concentration of 0.5 M CH_3OH. CV were recorded in the same way as in the case of ESA. To evaluate the activity, the following generally accepted parameters were used [5]: $Q_{CH3OH,}$ the amount of electricity used for the oxidation of methanol in the forward sweep of the potential; I_{max}, the maximum current density in the forward sweep of the potential, and $E_{initial}$, the potential for the oxidation onset of the direct anodic peak. To evaluate the tolerance of materials to CO, a chronoamperometry was used to evaluate the values of currents at the initial and final moment of the experiment. To do this, current decay curves were recorded at a constant potential of 0.6 V for 30 minutes. δ_{CO} coefficient

(coefficient of long-term CO poisoning) was used to express CO tolerance in quantitative terms [34]

TEM analysis of the catalysts' composition and microstructure was carried out using a FEI Tecnai G2 F20S-TWIN TMP microscope with an EDAX attachment operating at an accelerating voltage of 200 kV. Electrocatalyst powders (0.5 mg) were placed in 1 ml of heptane to prepare samples for TEM analysis. The suspension was then dispersed by ultrasound, after which a drop of suspension was applied to a copper grid coated with a thin layer of amorphous carbon. The eZAF (MThin) software algorithm implemented in the EDAX TEAM software was used to calculate the concentrations of the elements with due account of their peak intensities and the exit cross-section of their secondary X-ray emission for the lines of each element at each point of the map.

3. Results and discussion

To study the effect of the composition and structure of PtCo/C catalysts on their activity in the oxidation reaction of alcohols, liquid-phase synthesis was used to obtain PtCo/C catalysts of different mass fractions of the metal component and Pt:Co ratios. X-ray diffraction patterns of the obtained PtCo/C materials (Fig. 1) had peaks related to the phases of carbon C (002) and platinum Pt (111) and Pt (200). It should be noted that all reflections on the XRD patterns were characterised by a significant broadening, which is associated with the nanodispersed structure of the material. Also, all bimetallic materials were characterised by a shift of Pt (111) and Pt (200) peaks from the angles characteristic of the platinum phase (2θ = 39.8 and 46.3 degrees) towards higher values for angles 2θ. This fact is associated with a decreased lattice parameter (Table 1) due to the formation of solid Pt:Co and Pt:Ru solutions. The value of the crystal lattice parameter for solid solutions of the obtained PtCo/C materials was used to calculate the composition of solid Pt:Co solutions according to Vegard's law [35] (Table 1).

The XRD data with regard to reflection broadening and the Scherrer formula were used to calculate the average size of crystallites. As a result, for PC2, PC3, and JM20 catalysts, the calculated value was between 2.3 and 2.8 nm (Table 1), and for PtRu/C and PC1 catalysts it was 3.2 and 3.3 nm, respectively. According to the results of the XRF, the atomic metal ratios for all PtCo/C materials appeared to be close to those specified at the stage of synthesis (Table 1). However, it should be noted that the composition calculated according to Vegard's law differed significantly from the XRF data, which may be due to the incomplete entry of cobalt into the solid

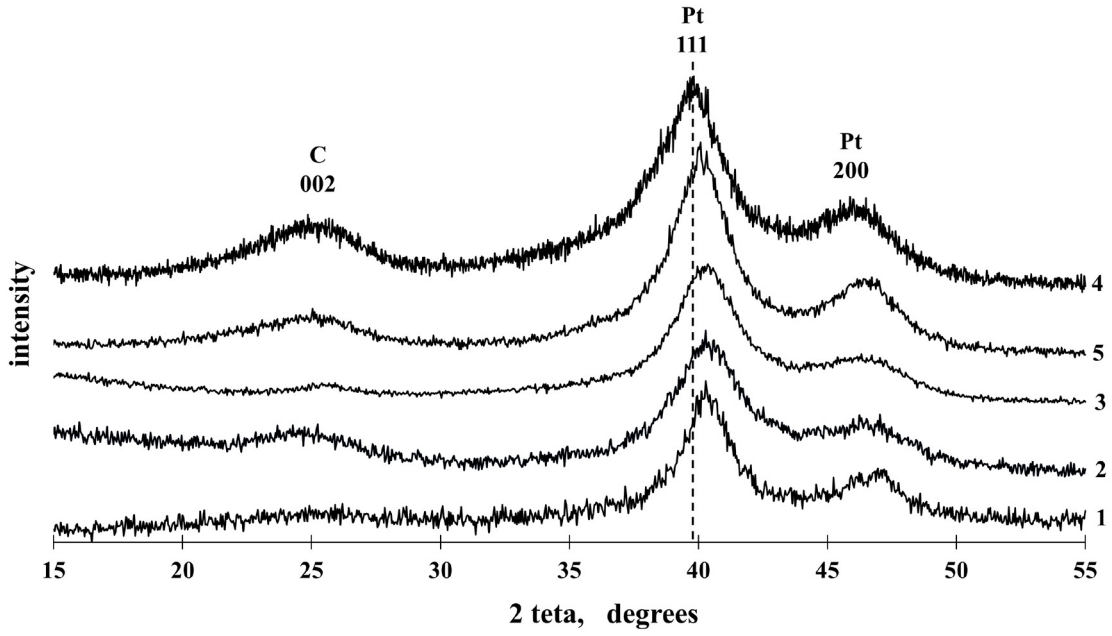

Fig. 1. X-ray diffraction patterns of platinum-containing materials: *1* – PC1; *2* – PC2; *3* – PC3; *4* – commercial Pt/C (JM20) sample; *5* – commercial PtRu/C sample

Table 1. Characteristics of PC materials obtained from CoO_x/C carriers

Materials	M-Loading (Pt), ω %	Metal Composition (According to XRF)	Metal Composition (According to XRD)	Lattice Parameter of the Metal Component, Å	Average crystallite size (XRD) Pt, nm
PC1	30±0.6	$Pt_{1.1}Co_1$	$Pt_{7.1}Co$	3.875	3.3±0.3
PC2	14±0.3	$Pt_{1.6}Co_1$	$Pt_{6.9}Co$	3.876	2.6±0.2
PC3	18±0.4	$Pt_{3.2}Co_1$	$Pt_{6.9}Co$	3.876	2.8±0.2
JM20	20±0.4	–	–	3.923	2.3±0.2
PtRu/C	40±0.8	Pt_1Ru_1	–	3.851	3.2±0.3

solution with platinum (Table 1). It should be noted that despite the difference in Pt:Co ratios in the obtained PtCo/C materials according to the XRF data, the amount of cobalt in the solid solution was almost the same and corresponded to the composition of Pt_7Co.

The microstructure and composition of PC1 and PC2 materials were also studied by TEM. In addition, the composition of the studied samples was studied by local EDAX microanalysis (Fig. 2). TEM images of the PC2 material (Fig. 2d, e) showed a uniform distribution of particles over the surface of the carbon carrier. The diameter of single particles was in the range from 1.5 to 3.5 nm. There were also a number of large agglomerates with a size of about 10 nm. The PC1 sample was characterised by particles with the size in the range from 3 to 5 nm (Fig. 2a, b), however, this material had a large number of large agglomerates of about 20 nm. The average size of metal nanoparticles for both PC1 and PC2 materials was slightly bigger than the average size of crystallites according to XRD data. It should be noted that it is typical for Pt/C and PtM/C materials to have a smaller average size of their crystallites according to XRD data than the size of metal nanoparticles according to TEM data, which can be due to a number of reasons [36].

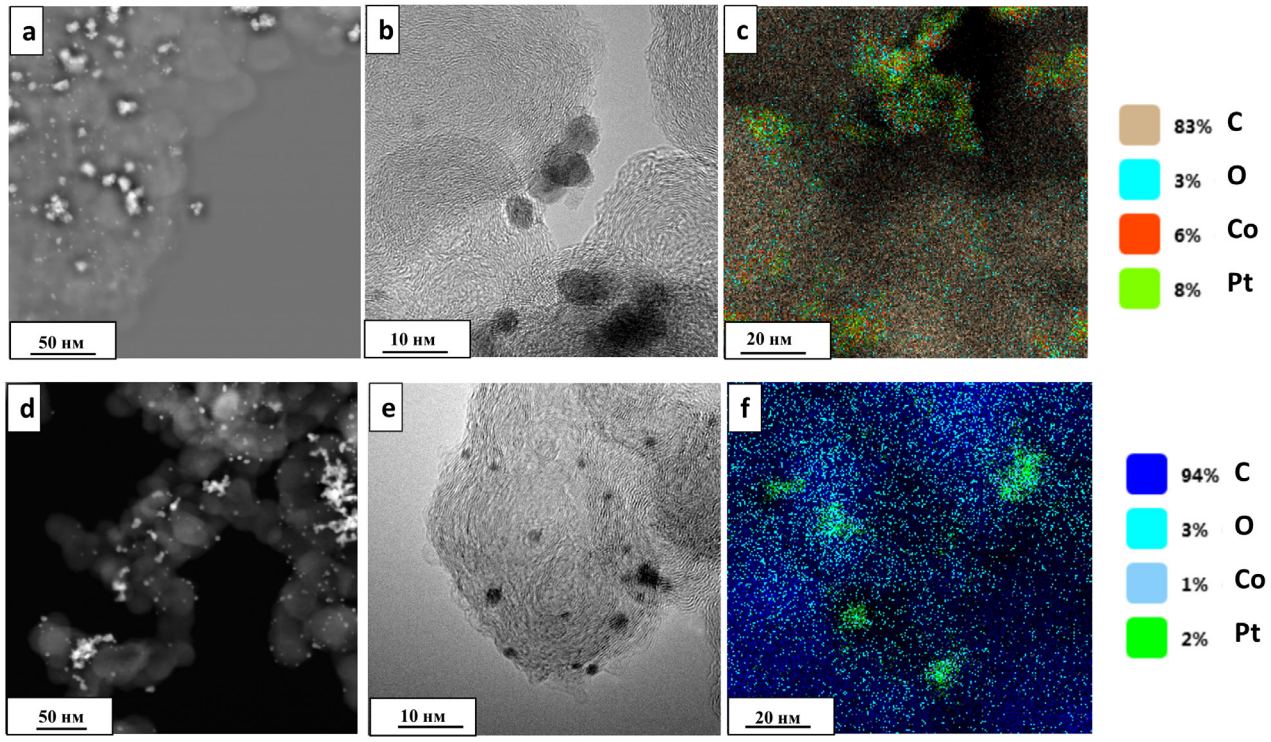

Fig. 2. TEM images of fragments of the material surface in PC1 (a, b), PC2 (d, e), and elemental mapping of fragments of PtCo/C surface in the PC1 (c), PC2 (e) samples

The results of elemental mapping of the surface fragments of the PC1 and PC2 materials indicated localisation of platinum and cobalt atoms in the same places (nanoparticles) (Fig. 2c, f), which also confirms the formation of bimetallic nanoparticles in the obtained materials. Local EDAX microanalysis used to determine the composition of the studied samples showed the atomic ratio of $PtCo_{1.27}$ and $PtCo_{1.05}$ for PC1 and PC2, respectively. These compositions were slightly different from the data received by the X-ray fluorescence analysis (Table 1), however, they confirmed a high content of cobalt in the obtained materials.

The CV of the obtained catalysts were characteristic of platinum-containing catalysts (Fig. 3). ESA values for all cobalt-containing catalysts determined by hydrogen adsorption/desorption were quite close (Table 2) and slightly lower than those of the commercial JM20 sample. ESA values for PC materials were quite high and exceeded or corresponded to the materials described in [12, 37]. It should be noted that it is difficult to determine the area for PtRu/C catalysts by this method [38-39], therefore, the method of the oxidation of a chemisorbed CO monolayer was used to determine the surface area for all materials. ESA values determined by CO oxidation (Fig. 3b), which was carried out for all catalysts, are in good agreement with the data obtained for hydrogen adsorption/desorption (Table 2). Several maximums on the CO oxidation voltammogrammes may be caused by several factors , such as the formation of alloys of different compositions [40–41], the influence of various faces of platinum [42], and defects on the platinum faces [43]. All these factors may also apply to the obtained PtCo/C materials. It should

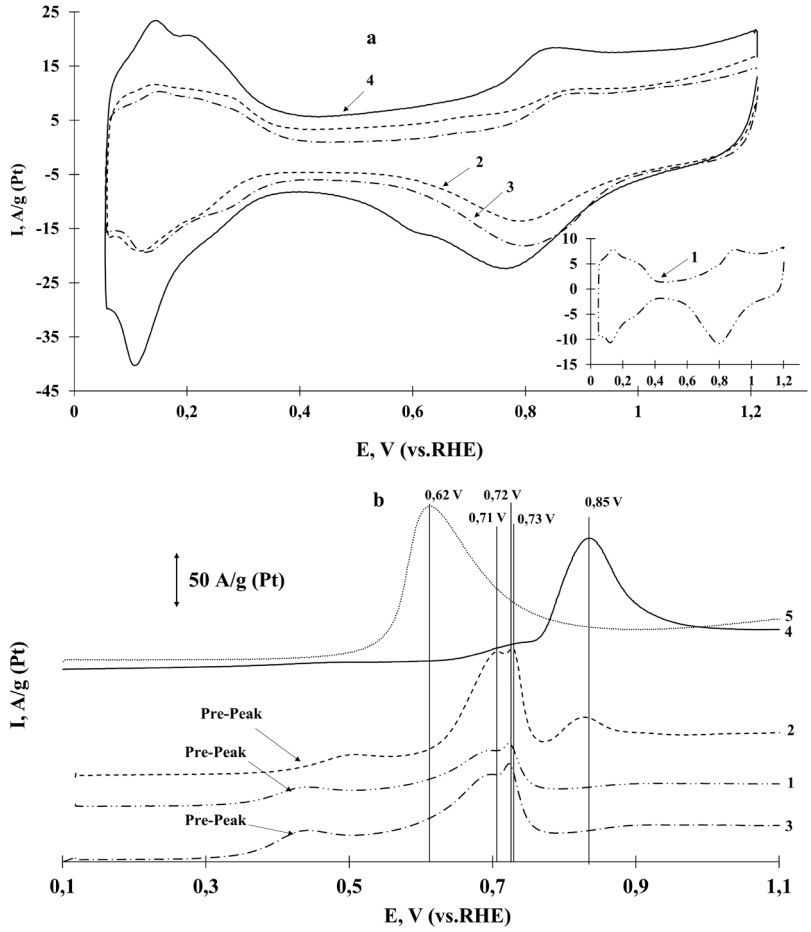

Fig. 3. Cyclic voltammogrammes (2nd cycle) (a) and fragments of cyclic voltammogrammes, including peaks of CO electrochemical desorption from the surface of nanoparticles of the studied catalysts (b): *1* – PC1; *2* – PC2; *3* – PC3; *4* – commercial Pt/C (JM20) sample; *5* – commercial PtRu/C sample. Electrolyte is 0.1 M $HClO_4$, argon atmosphere. Potential sweep rate is 40 mV/s

Table 2. Parameters characterising the electrochemical behaviour of catalysts in MOR

Materials	ESA		I_{max}, A/g (Pt, PtRu)	$E_{initial}$, V	*I* chronoamperograms, A/g (Pt, PtRu)		δ_{CO}, %/s
	$H_{ads/des}$ $m^2/g(Pt)$	CO $m^2/g(Pt)$			$I_{initial}$ *	I_{final}	
PC1	52±5	45±5	563	0.57	19.3	9.5	0.039
PC2	51±5	58±5	849	0.54	32.6	17.4	0.036
PC3	53±5	47±5	834	0.55	35.4	16.6	0.041
JM20	75±7	76±7	401	0.58	20.5	17.2	0.012
PtRu/C	–	80±8	218	0.52	47.8	26.3	0.034

* – values 10 seconds after the start of the experiment.

be noted that CO oxidation for all bimetallic PtCo/C catalysts started at less positive potentials than for the commercial Pt/C material and at more positive potentials as compared to PtRu/C. At the same time, PtCo/C catalysts had a pronounced prepeak at potentials of 0.4–0.5 V. According to Petry's review [44], prepeaks in the range of potentials of 0.35–0.6 V are usually associated with the CO_{ads} oxidation in the defective sites of metal surfaces. This indirectly indicates a greater tolerance of the obtained bimetallic systems to CO poisoning as compared to the Pt/C material and makes them potentially very promising catalysts for oxidation reactions of organic substances in which CO is one of the intermediate products of the oxidation reaction [6].

The activity of the obtained catalysts in MOR was determined by the parameters of the direct peak of methanol oxidation on CV (Fig. 4a). The direct peak (0.7–1 V) was due to the oxidation of methanol molecules and their intermediates on the clean surface of platinum-containing catalysts. The PC2 and PC3 catalysts were characterised by the highest currents at the maximum, 849 and 834 A/g, respectively, which exceeded this parameter for the PC1 catalyst by 1.48 times and for the commercial JM20 and PtRu/C catalysts by 2.0 and 3.8 times. Such results correlate well with the data provided by the authors in [45]. It should be noted that PtRu/C had the lowest potential for the oxidation onset, which also indicated that it was the most active in MOR. $E_{initial}$ values for all PC materials were very close and were within the range of 0.54 to 0.57 V, which was lower than for the commercial JM20 catalyst (Table 2; Fig. 4b). From the forward sweep section of cyclic voltammogrammes, it is obvious that the PC2 material had the highest activity in the potential range of 0.6 – 0.8 V. The PtRu/C and PC1 samples had the lowest current values at a potential of 0.6 V (Fig. 4B, inset), while the PC1 sample at potentials of 0.7 and 0.8 V was characterised by more than 2 times higher currents than the PtRu/C catalyst. An increased activity of PtCo/C materials in the MOR reaction as compared to Pt/C can be associated with both the size of metal nanoparticles and the structure of the active component and with the doping of platinum with cobalt. It should be noted that the effect of doping platinum with cobalt must not be excluded despite cobalt elution from the surface of nanoparticles. As mentioned in [45-48], the introduction of cobalt reduces the parameter of the crystal lattice and leads to a decrease in the energy of the *d*-sublevel, which leads to an increase in catalytic activity. These effects are still observed after cobalt elution from the surface of nanoparticles.

A comprehensive study of the characteristics of the studied catalysts in the oxidation reaction of alcohols requires chronoamperometric measurements at potentials close to the potential of the methanol oxidation onset, in this case at a potential of 0.6 V (Fig. 5). The highest values of $I_{initial}$ and I_{final} were characteristic of the PtRu/C catalyst. This fact agrees with the onset of CO oxidation at less positive potentials as compared to the other studied catalysts (Fig. 3). As for PC materials, the highest characteristics were shown by materials with a close mass fraction: 14 and 18 %. It should be noted that there was no dependence of the catalysts' characteristics in MOR on the catalysts' composition possibly due to the same composition of the solid PtCo solution according to XRD. What is more, the PC1 sample, which was characterised by the

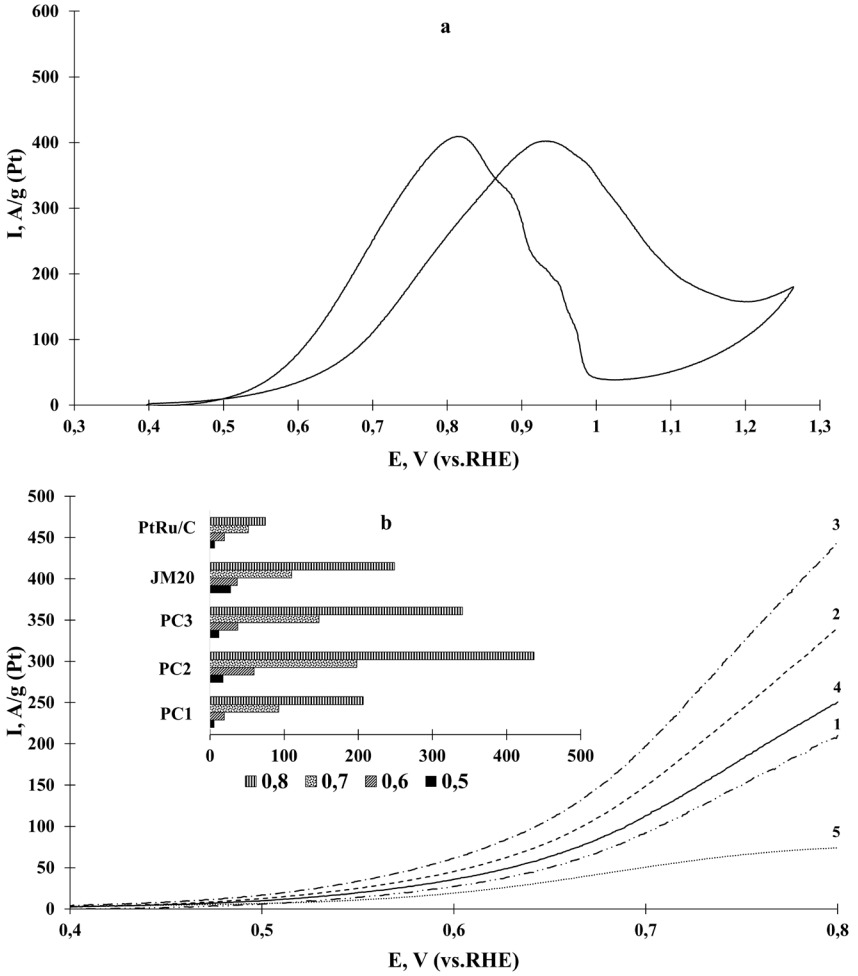

Fig. 4. Typical CV (a) and the forward sweep section of cyclic voltammogrammes in the range of potentials between 0.4 and 0.8 V (b), the values of specific currents at certain potentials (inset) for: *1* – PC1; *2* – PC2; *3* – PC3; *4* – JM20; *5* – commercial PtRu/C sample. Currents are normalised to the Pt or PtRu mass. Electrolyte is 0.1 M $HClO_4$ with 0.5 M CH_3OH. Ar atmosphere

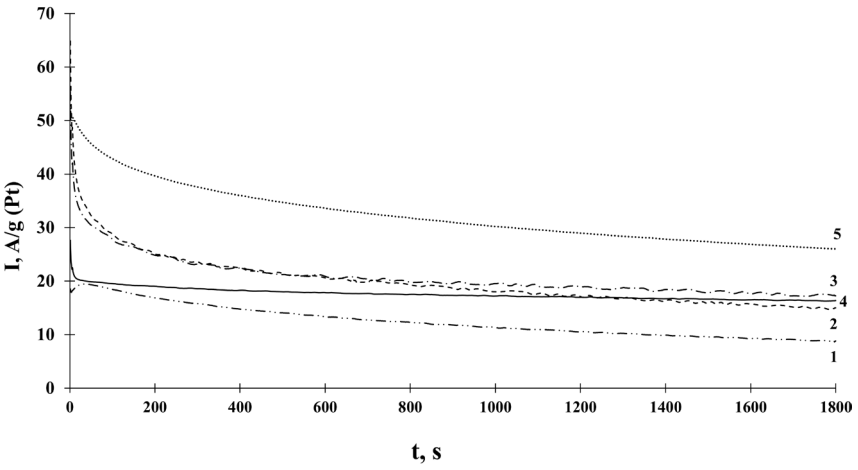

Fig. 5. Chronoamperogrammes at a potential of 0.6 V for: *1* – PC1; *2* – PC2; *3* – PC3; *4* – JM20; *5* – commercial PtRu/C sample. Currents are normalised to the Pt or PtRu mass. Electrolyte is 0.1 M $HClO_4$ with 0.5 M CH_3OH. Ar atmosphere

value of I_{on} close to that of the JM20 sample, degraded much more in 30 minutes and the value I_{fin} for PC1 was almost 2 times lower than for the commercial Pt/C catalyst (Fig. 5). The delta value shows the degree of material degradation during chronopotentiometry measurements. According to this value, the most stable material is the commercial Pt/C material (δ = 0.012). The other catalysts had significantly higher δ values than those of the JM20 catalyst, which indicates lower stability of both PtCo/C and PtRu/C catalysts. However, since the absolute values of I_{initial} and I_{final} for PtRu/C were higher than those for JM20, this means that this catalyst is more promising.

Hence, it can be concluded that according to chronoamperometry data and the potential for the onset of CO oxidation, the most active catalyst in MOR is the commercial PtRu/C catalyst. However, PC2 and PC3 PtCo/C materials are much more superior to the commercial Pt/C catalyst. The analysis of voltampreometry data for PtCo/C materials of the PC series revealed that they have higher characteristics at potentials above 0.5 V as compared to the commercial materials. These differences are due to the peculiarities of the methods. For example, CV data records curves with a high sweep rate, which allows assessing the activity of catalysts and their tolerance to CO. When measuring chronoamperometry, the system is observed until it reaches stationary currents, which provides information allowing to evaluate the stability of electrocatalysts and their poisoning by chemisorbed reaction products [49, 50].

Similar methods were used to study the activity of all obtained catalysts in EOR. According to cyclic voltammetry data (Fig. 6b), it can be concluded that the E_{initial} value for PC materials is less positive as compared to commercial catalysts, which confirms the high activity of these catalysts

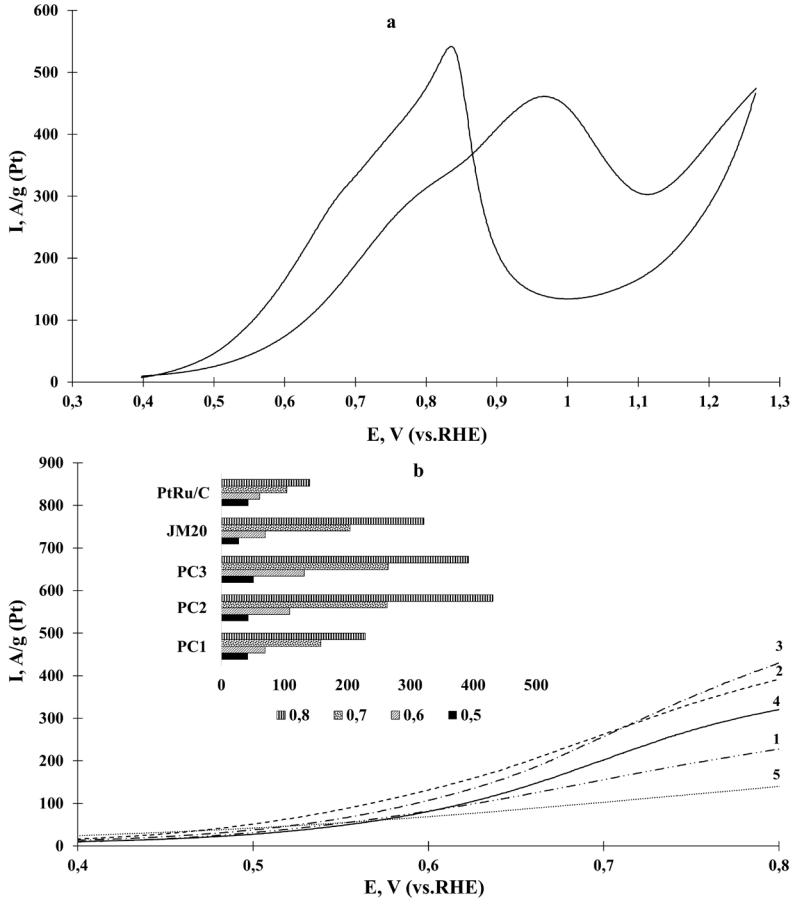

Fig. 6. Typical cyclic voltammogrammes (a) and the forward sweep section of cyclic voltammogrammes in the range of potentials between 0.4 and 0.8 V (b), the values of currents at certain potentials (inset) for: *1* – PC1; *2* – PC2; *3* – PC3; *4* – JM20; *5* – commercial PtRu/C sample. Currents are normalised to the Pt or PtRu mass. Electrolyte is 0.1 M $HClO_4$ with 0.5 M C_2H_5OH. Ar atmosphere

in EOR (Table 3). At the same time, $E_{initial}$ values for all PC materials are quite close. In the case of EOR, the I_{max} value was 1.5 to 3.7 times higher for the PC2 sample than for all studied samples. It should also be noted that for the PC1 and PC3 materials, the I_{max} values were higher than for the commercial PtRu/C and JM20 catalysts (Table 3).

The analysis of the forward sweep sections of cyclic voltammogrammes in EOR allowed concluding that all catalysts but JM20 had high current values at a potential of 0.5 V. With further growth of potentials, there is a tendency to a sharp increase in currents for all PtCo/C catalysts of the PC series (Fig. 6b, inset).

According to the results of chronoamperometric (Fig. 7) measurements, the highest values of $I_{initial}$ and I_{final} were characteristic of the PC2 and PC3 materials. The PC2 material is characterised by the lowest value of δ, which indicates the highest stability of this material. It is important to emphasise that the PtRu/C catalyst exhibited characteristics close to the PC1 catalyst and inferior characteristics than the PC2 and PC3 materials. The JM20 catalyst, in turn, demonstrated the most inferior characteristics among all the studied materials.

The superior characteristics of the obtained PtCo/C materials as compared to the commercial PtRu/C sample in MOR can apparently be explained by a decreased crystal lattice parameter and electronic effects on the surface of nanoparticles caused by the influence of the subsurface solid PtCo solution [50, 51]. These effects lead to a decrease in the energy of the Pt *d*-sublevel. They reduce the adsorption of intermediate poisoning products on the surface of Pt and contribute to their easier removal from the surface [51, 52].

4. Conclusions

We studied the possibility of using PtCo/C materials of various compositions for the methanol and ethanol oxidation reaction. It was found that the samples of PtCo/C catalysts with a close mass fraction of platinum of 14 and 18%

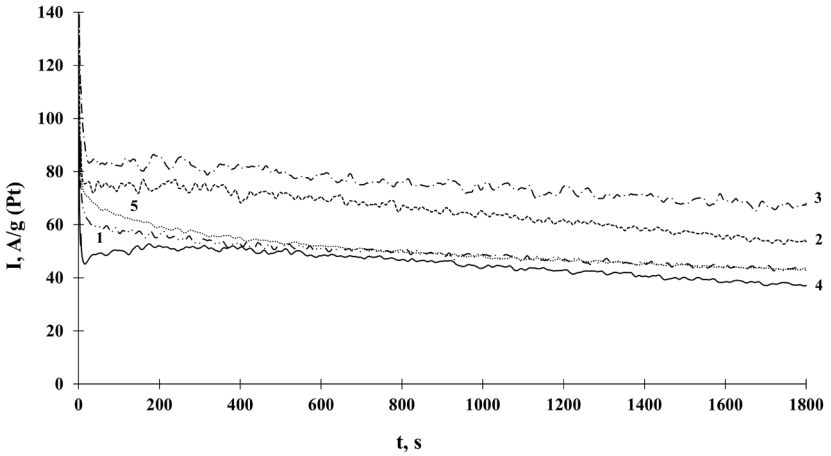

Fig. 7. Chronoamperogrammes at a potential of 0.6 V for: *1* – PC1; *2* – PC2; *3* – PC3; *4* – JM20; *5* – commercial PtRu/C sample. Currents are normalised to the Pt or PtRu mass. Electrolyte is 0.1 M $HClO_4$ with 0.5 M C_2H_5OH. Ar atmosphere

Table 3. Parameters characterising the electrochemical behaviour of catalysts in EOR

Materials	I_{max}, A/g (Pt, PtRu)	$E_{initial}$, V	*I* chronoamperograms, A/g (Pt, PtRu)		δ_{CO}, %/c
			$I_{initial}$*	I_{final}	
PC1	460	0.53	61.6	43.6.	0.022
PC2	867	0.54	83.4	67.6	0.015
PC3	563	0.52	75.3	53.6	0.022
JM20	454	0.58	48.0	37.3	0.017
PtRu/C	234	0.59	68.7	43.7	0.027

* – values 10 seconds after the start of the experiment

and different compositions of PtCo/C and Pt_3Co/C are characterised by similar values of activity and stability in both EOR and MOR. Increased volume of platinum in the PtCo/C material has a negative impact on the catalyst's characteristics in MOR and EOR. For example, the values of I_{max} for the PC1 sample are the lowest among all PtCo/C samples and the values of currents in the range of potentials of 0.5 to 0.8 V are about 2 times lower in MOR and 1.5 times lower in EOR. According to the comparative analysis of the commercial Pt/C and PtRu/C catalysts in the methanol oxidation reaction, the most active and stable catalyst by a combination of chronoamperometry data and $E_{initial}$ values is the PtRu/C catalyst. In the case of ethanol oxidation reaction, the PC2 and PC3 samples of PtCo/C are superior to commercial samples in all of the studied parameters. Considering the combination of characteristics of PtCo/C materials, we conclude that further research of cobalt-containing catalysts can open new opportunities for alcohol fuel cells.

Contribution of the authors

The authors contributed equally to this article.

Conflict of interests

The authors declare that they have no known competing financial interests or personal relationships that could have influenced the work reported in this paper.

References

1. Sundarrajan S., Allakhverdiev S. I., Ramakrishna. S. Progressand perspectives in micro direct methanol fuel cell. *Int J of Hydrogen Energy*. 2012;37(10): 8765–8786. https://doi.org/10.1016/j.ijhydene.2011.12.017

2. Yaroslavtsev A. B., Dobrovolsckiy Yu. A., Shaglaeve N. S., Frolova L. A., Gerasimova E. V., Sanginov E. A. Nanostructured materials developed for the low temperature fuel elements, *Russian Chemical Reviews*. 2012;81(3) 191–201. https://doi.org/10.1070/RC2012v081n03ABEH004290

3. Karim N. A., Kamarudin S. K. Introduction to direct alcohol fuel cells (DAFCs). *Direct Liquid Fuel Cells*. 2021: 49–70. https://doi.org/10.1016/B978-0-12-818624-4.00002-9

4. Wang X. X., Swihart M. T., Wu G. Achievements, challenges andperspectives on cathode catalysts in proton exchangemembrane fuel cells for transportation. *Nature Catalysis*. 2019;2: 578–589. https://doi.org/10.1038/s41929-019-0304-9

5. Menshikov V. S., Novomlinsky I. N., Belenov S. V., Alekseenko A. A., Safronenko O. I., Guterman V. E. Methanol, ethanol, and formic acid oxidation on new platinum-containing catalysts. *Catalysts*. 2021;11: 1–18. https://doi.org/10.3390/catal11020158

6. Petrii O. A. The progress in understanding the mechanisms of methanol and formic acid electrooxidation on platinum group metals. *Russian Journal of Electrochemistry*. 2019;55: 1-33. https://doi.org/10.1134/S1023193519010129

7. Vigier F., Coutanceau C., Hahn F., Belgsir E. M., Lamy, C. On the mechanism of ethanol electro-oxidation on Pt and PtSn catalysts: electrochemical and in situ IR reflectance spectroscopy studies. *Journal of Electroanalytical Chemistry*. 2004;563(1): 81–89. https://doi.org/10.1016/j.jelechem.2003.08.019

8. Chen A., Holt-Hindle P. Platinum-based nanostructuredmaterials properties, and applications. *Chemical Reviews*. 2010;110(6): 3767–3804. https://doi.org/10.1021/cr9003902

9. Shi G. Y., Yano H., Tryk D. A., Watanabe M., Uchida H. A novel Pt–Co alloy hydrogen anode catalyst with superlative activity, CO-tolerance and robustness. *Nanoscale*. 2016;8: 13893–13897. https://doi.org/10.1039/c6nr00778c

10. Antolini E., Salgado J. R. C., Gonzalez E. R. The methanol oxidation reaction on platinum alloys with the first row transition metals: The case of Pt-Co and -Ni alloy electrocatalysts for DMFCs: A short review. *Applied Catalysis B: Environmental*. 2006;63(1–2): 137–149. https://doi.org/10.1016/j.apcatb.2005.09.014

11. Baronia R., Goel J., Tiwari S., Singh P. Efficient electro-oxidation of methanol using PtCo nanocatalysts supported reduced graphene oxide matrix as anode for DMFC. *International Journal of Hydrogen Energy*. 2017;42(15): 10238–10247. https://doi.org/10.1016/j.ijhydene.2017.03.011

12. Xu Y., Yuan Y., Ma A., Wu X., Liu Y., Zhang B. Composition-tunable Pt-Co alloy nanoparticle networks: facile room-temperature synthesis and supportless electrocatalytic applications. *ChemPhysChem*. 2012;13: 2601–2609. https://doi.org/10.1002/cphc.201100989

13. Sorsa O., Romar H., Lassi U., Kallio T. Co-electrodeposited mesoporous PtM (M=Co, Ni, Cu) as an active catalyst for oxygen reduction reaction in a polymer electrolyte membrane fuel cell. *Electrochimica Acta*. 2017;230: 49–57. https://doi.org/10.1016/j.electacta.2017.01.158

14. Mohl M., Dobo D., Kukovecz A., … Ajayan P. M. Formation of CuPd and CuPt bimetallic nanotubes by galvanic replacement reaction. *The Journal of Physical Chemistry C*. 2011;115: 9403–9409. https://doi.org/10.1021/jp112128g

15. Wang X., Zhang L., Wang F., Yu J., Zhu H. Nickel-introduced structurally ordered PtCuNi/C as high performance electrocatalyst for oxygen reduction reaction. *Progress in Natural Science: Materials Inter-*

national. 2020;30(6): 905–911. https://doi.org/10.1016/j.pnsc.2020.10.017

16. Asset T., Chattot R., Fontana M., … Maillard F. A Review on recent developments and prospects for the oxygen reduction reaction on hollow Pt-alloy nanoparticles. *ChemPhysChem*. 2018;19: 1552–1567. https://doi.org/10.1002/cphc.201800153

17. Jalan V. M., Taylor E. J. Importance of interatomic spacing in catalytic reduction of oxygen in phosphoric acid. *Journal of The Electrochemical Society*. 1983;130(11): 2299–2302. https://doi.org/10.1149/1.2119574

18. Toda T., Igarashi H., Uchida H., Watanabe M. Enhancement of the electroreduction of oxygen on Pt Alloys with Fe, Ni, and Co. *Journal of The Electrochemical Society*. 1999;146: 3750–3756. https://doi.org/10.1149/1.1392544

19. Munoz M., Ponce S., Zhang G. R., Etzold B. J. M. Size-controlled PtNi nanoparticles as highly efficient catalyst for hydrodechlorination reactions. *Applied Catalysis B: Environmental*. 2016;192: 1–7. https://doi.org/10.1016/J.APCATB.2016.03.038

20. Konno N., Mizuno S., Nakaji H., Ishikawa Y. Development of compact and high- performance fuel cell stack. *SAE International Journal of Alternative Powertrains*. 2015;4(1): 123–129. https://doi.org/10.4271/2015-01-1175

21. Ding J., Ji S., Wang H., Pollet B. G., Wang R. Tailoring nanopores within nanoparticles of PtCo networks as catalysts for methanol oxidation reaction. *Electrochimica Acta*. 2017;255: 55–62. https://doi.org/10.1016/j.electacta.2017.09.159

22. Li Z., Jiang X., Wang X., … Tang Y. Concave PtCo nanocrosses for methanol oxidation reaction. *Applied Catalysis B: Environmental*. 2020;270: 119135–119160. https://doi.org/10.1016/j.apcatb.2020.119135

23. Xu C., Hou J., Pang X., Li X., Zhu M., Tang B. Nanoporous PtCo and PtNi alloy ribbons for methanol electrooxidation. *International Journal of Hydrogen Energy*. 37(14), 10489–10498. https://doi.org/10.1016/j.ijhydene.2012.04.041

24. Flórez-Montaño J., García G., Guillén-Villafuerte O., Rodríguez J. L., Planes G. A., Pastor E. Mechanism of ethanol electrooxidation on mesoporous Pt electrode in acidic medium studied by a novel electrochemical mass spectrometry set-up. *Electrochimica Acta*. 2016;209: 121–131. https://doi.org/10.1016/j.electacta.2016.05.070

25. Bonesi A., Garaventa G., Triaca W., Castro Luna A. Synthesis and characterization of new electrocatalysts for ethanol oxidation. *International Journal of Hydrogen Energy*. 2008;33(13): 3499–3501. https://doi.org/10.1016/j.ijhydene.2007.12.056

26. Parreira L. S., Antoniassi R. M., Freitas I. C., de Oliveira D. C., Spinacé E. V., Camargo P. H. C., dos Santos M. C. MWCNT-COOH supported PtSnNi electrocatalysts for direct ethanol fuel cells: Low Pt content, selectivity and chemical stability. *Renewable Energy*. 2019;143: 1397–1405. https://doi.org/10.1016/j.renene.2019.05.067

27. Li J., Jilani S. Z., Lin H., … Sun S. Ternary CoPtAu nanoparticles as a general catalyst for highly efficient electro-oxidation of liquid fuels. *Angewandte Chemie*. 2019;*131*(33): 11651–11657. https://doi.org/10.1002/ange.201906137

28. Xu C., Su Y., Tan L., Liu Z., Zhang J., Chen S., Jiang S. P. Electrodeposited PtCo and PtMn electrocatalysts for methanol and ethanol electrooxidation of direct alcohol fuel cells. *Electrochimica Acta*. 2009;54(26): 6322–6326. https://doi.org/10.1016/j.electacta.2009.05.088

29. Kepenienė V., Tamašauskaitė-Tamašiūnaitė L., Jablonskienė J., Vaičiūnienė J., Kondrotas R., Juškėnas R., Norkus E. Investigation of graphene supported platinum-cobalt nanocomposites as electrocatalysts for ethanol pxidation. *Journal of The Electrochemical Society*. 2014;161(14): F1354–F1359. https://doi.org/10.1149/05901.0217ecst

30. Mondal A., De A., Datta J. Selective methodology for developing PtCo NPs and performance screening for energy efficient electro-catalysis in direct ethanol fuel cell. *International Journal of Hydrogen Energy*. 2019;44(21): 10996–11011. https://doi.org/10.1016/j.ijhydene.2019.02.146

31. Zhai X., Wang P., Wang K., Li J., Pang X., Wang X., Li Z. Facile synthesis of PtCo nanowires with enhanced electrocatalytic performance for ethanol oxidation reaction. *Ionics*. 2020;26(6): 3091–3097. https://doi.org/10.1007/s11581-019-03419-1

32. Mauer D., Belenov S., Guterman V., … Safronenko O. Gram-scale synthesis of CoO/C as base for PtCo/C high-performance catalysts for the oxygen reduction reaction. *Catalysts*. 2021;11(12): 1539–1558. https://doi.org/10.3390/catal11121539

33. Langford J. I., Wilson A. J. C. Scherrer after sixty years: a survey and some new results in the determination of crystallite size. *Journal of Applied Crystallography*. 1978;11(2): 102–103. https://doi.org/10.1107/S0021889878012844

34. Guo J. W., Zhao T. S., Prabhuram J., Chen R., Wong C.W. Preparation and characterization of a PtRu/C nanocatalyst for direct methanol fuel cells. *Electrochimica Acta*. 2005;51(4): 754–763. https://doi.org/10.1016/j.electacta.2005.05.056

35. Jenkins R., Snyder R. L. *Introduction to X-Ray powder diffractometry*. John Wiley & Sons; 1996. 432 p.

36. Favilla P. C., Acosta J. J., Schvezov C. E., Sercovich D. J., Collet-Lacos J. R. Size control of carbon-supported platinum nanoparticles made using polyol method for low temperature fuel cells. *Chemical Engineering Science*. 2013;101: 27–34. https://doi.org/10.1016/j.ces.2013.05.067

37. Hu S., Wang Z., Chen H., Wang S., Li X., Zhang X., Shen P. K. Ultrathin PtCo nanorod assemblies with self-optimized surface for oxygen reduction reaction. *Journal of Electroanalytical Chemistry*. 2020;870, 114194–114201. https://doi.org/10.1016/j.jelechem.2020.114194

38. Huang T., Zhang D., Xue L., Cai W.-B., Yu A. A facile method to synthesize well-dispersed PtRuMoOx and PtRuWOx nanoparticles and their electrocatalytic activities for methanol oxidation. *Journal of Power Sources*. 2009;192(2): 285–290. https://doi.org/10.1016/j.jpowsour.2009.03.037

39. Kuo C.-W., Lu I-T., Chang L.-C., … Lee J.-F. Surface modification of commercial PtRu nanoparticles for methanol electro-oxidation. *Journal of Power Sources*. 2013;240: 122–130. https://doi.org/10.1016/j.jpowsour.2013.04.001

40. Rudi S., Cui C., Gan L., Strasser P. Comparative study of the electrocatalytically active surface Aareas (ECSAs) of Pt alloy nanoparticles evaluated by H_{upd} and CO-stripping voltammetry. *Electrocatalysis*. 2014;5: 408–418. https://doi.org/10.1007/s12678-014-0205-2

41. Van der Vliet D. F., Wang C., Li D., … Stamenkovic V. R. Unique electrochemical adsorption properties of Pt-skin surfaces. *Angewandte Chemie International Edition*. 2012;51(3): 3139–3142. https://doi.org/10.1002/anie.201107668

42. de la Fuente J. L. G., Rojas S., Martínez-Huerta M. V., Terreros P., Peña M. A., Fierro J. L. G. Functionalization of carbon support and its influence on the electrocatalytic behaviour of Pt/C in H_2 and CO electrooxidation. *Carbon*. 2006;44: 1919–1929. https://doi.org/10.1016/j.carbon.2006.02.009

43. Travitsky N., Ripenbein T., Golodnitsky D., Rosenberg Y., Burshtein L., Peled E. Pt-, PtNi- and PtCo-supported catalysts for oxygen reduction in PEM fuel cells. *Journal of Power Sources*. 2006;161: 782–789. https://doi.org/10.1016/j.jpowsour.2006.05.035

44. Li X., Liu Y., Zhu J., Tsiakaras P., Shen P. K. Enhanced oxygen reduction and methanol oxidation reaction over self-assembled Pt-M (M = Co, Ni) nanoflowers. *Journal of Colloid and Interface Science*. 2022;607: 1411–1423. https://doi.org/10.1016/j.jcis.2021.09.060

45. Yang H. Platinum-based electrocatalysts with core-shell nanostructures. *Angewandte Chemie International Edition*. 2011;50(12): 2674. https://doi.org/10.1002/anie.201005868

46. Paulus U. A., Wokaun A., Scherer G. G., Schmidt T. J., Stamenković V., Marković N. M., Ross P. N. Oxygen reduction on high surface area Pt-based alloy catalysts in comparison to well defined smooth bulk alloy electrodes. *Electrochimica Acta*. 2002;47(22-23): 3787. https://doi.org/10.1016/s0013-4686(02)00349-3

47. Xing Z., Li J., Wang S., Su C., Jin H. Structure engineering of $PtCu_3$/C catalyst from disordered to ordered intermetallic compound with heat-treatment for the methanol electrooxidation reaction. *Nano Research*. 2022;15: 3866–3871. https://doi.org/10.1007/s12274-021-3993-8

48. Petrii O. A. Pt–Ru electrocatalysts for fuel cells: a representative review. *Journal of Solid-State Electrochemistry*. 2008;12(5): 609–642. https://doi.org/10.1007/s10008-007-0500-4

49. Tolmachev Y. V., Petrii O. A. Pt–Ru electrocatalysts for fuel cells: developments in the last decade. *Journal of Solid-State Electrochemistry*. 2017;21: 613–639. https://doi.org/10.1007/s10008-016-3382-5

50. Castagna R. M., Sieben J. M., Alvarez A. E., Duarte M. M. E. Electrooxidation of ethanol and glycerol on carbon supported PtCu nanoparticles. *International Journal of Hydrogen Energy*. 2019;44: 5970–5982. https://doi.org/10.1016/j.ijhydene.2019.01.090

51. Fang B., Feng L. PtCo-NC catalyst derived from the pyrolysis of Pt-incorporated ZIF-67 for alcohols fuel electrooxidation. *Acta Physico-Chimica Sinica*. 2020;36(7): 1905023. https://doi.org/10.3866/PKU.WHXB201905023

Information about the authors

Dmitry D. Mauer, Researcher at the Department of Electrochemistry, Southern Federal University (Rostov-on-Don, Russian Federation).
https://orcid.org/0000-0002-1658-2426
dima333000@yandex.ru

Sergey V. Belenov, Cand. Sci. (Chem.), Research Fellow at the Department of Electrochemistry, Southern Federal University (Rostov-on-Don, Russian Federation).
https://orcid.org/0000-0003-2980-7089
serg1986chem@mail.ru

Aleksey Y. Nikulin, Researcher at the Department of Electrochemistry, Southern Federal University (Rostov-on-Don, Russian Federation).
chemistnik@yandex.ru

Toporkov N. Vasilyevich, trainee researcher, Research Institute of Physics Department of Analytical Instrumentation, Southern Federal University (Rostov-on-Don, Russian Federation).
ntoporkov@sfedu.ru.

Received 15.08.2022; approved after reviewing 21.11.2022; accepted for publication 15.12.2022; published online 25.03.2023.

Translated by Irina Charychanskaya
Edited and proofread by Simon Cox